

# Mid-infrared guided optics: a perspective for astronomical instruments

Lucas Labadie,<sup>1\*</sup> and Oswald Wallner<sup>2</sup>

<sup>1</sup>Max-Planck Institut fuer Astronomie, Koenigstuhl 17, D-69117 Heidelberg, Germany

<sup>2</sup>EADS Astrium GmbH, 88039 Friedrichshafen, Germany

\* Corresponding author: [labadie@mpia.de](mailto:labadie@mpia.de)

**Abstract:** Research activities during the last decade have shown the strong potential of photonic devices to greatly simplify ground based and space borne astronomical instruments and to improve their performance. We focus specifically on the mid-infrared wavelength regime (about 5–20  $\mu\text{m}$ ), a spectral range offering access to warm objects (about 300 K) and to spectral features that can be interpreted as signatures for biological activity (e.g. water, ozone, carbon dioxide). We review the relevant research activities aiming at the development of single-mode guided optics and the corresponding manufacturing technologies. We evaluate the experimentally achieved performance and compare it with the performance requirements for applications in various fields of astronomy. Our goal is to show a perspective for future astronomical instruments based on mid-infrared photonic devices.

© 2018 Optical Society of America

**OCIS codes:** (130.3060) Infrared; (130.3120) Integrated optics devices; (130.3130) Integrated optics materials; (350.1270) Astronomy and astrophysics; (060.2430) Fibers, single-mode; (060.5295) Photonic crystal fibers; (060.2390) Fiber optics, infrared

---

## References and links

1. V. Coudé du Foresto, G. Perrin, J.-M. Mariotti, M. Lacasse and W. Traub, in *The FLUOR/IOTA fiber stellar interferometer*, F. Malbet, P. Kern, eds. (Bastianelli-Guirimand, 1997), pp.115–125.
2. H. A. McAlister, T. A. ten Brummelaar, L. Sturmman, J. Sturmman, N. H. Turner and S. T. Ridgway, “Recent progress at the CHARA interferometric array,” *Proc. SPIE* **6268**, 62680G (2006).
3. R. Petrov, F. Malbet and G. Weigelt, “AMBER, the near-infrared spectro-interferometric three-telescope VLTI instrument,” *Astron. Astrophys.* **464**, 1–12 (2007).
4. G. Perrin, J. Woillez, O. Lai, J. Guérin, T. Kotani, P. L. Wizinowich, D. Le Mignant, M. Hrynevych, J. Gathright, P. Léna F. Chaffee and S. Vergnole, “Interferometric coupling of the Keck telescopes with single-mode fibers,” *Science* **311**, 194 (2006).
5. J.-P. Berger, P. Haguenuer, P. Kern, K. Perraut, F. Malbet, I. Schanen, M. Severi, R. Millan-Gabet and W. Traub, “Integrated optics for astronomical interferometry. IV. First measurements of stars,” *Astron. Astrophys. Suppl. Ser.* **376**, L31–L34 (2001).
6. F. P. Schloerb, J.-P. Berger, N. P. Carleton and P. Hagenauer, “IOTA: recent science and technology,” *Proc. SPIE* **6268**, 62680I (2006).
7. F. Malbet, J.-P. Berger, P. Garcia, P. Kern, K. Perraut, M. Benisty, L. Jocou, E. Herwats, J.-B. Lebouquin, P. Labeye, E. Le Coarer and O. Preis, “VITRUV - Imaging close environments of stars and galaxies with the VLTI at milli-arcsec resolution,” in *The Power of Optical/IR Interferometry: Recent Scientific Results and 2nd Generation VLTI Instrumentation*, A. Richichi, F. Delplancke, F. Paresce, A. Chelli, eds. (Springer, 2008), pp.357–369.
8. F. Eisenhauer, G. Perrin, W. Brandner, C. Straubmeier and A. Richichi, “GRAVITY: getting to the event horizon of Sgr A\*,” *Proc. SPIE* **7013**, 70132A (2008).
9. J. Bland-Hawthorn and A. Horton, “Instruments without optics: an integrated photonic spectrograph,” *Proc. SPIE* **6269**, 62690N (2008).
10. E. Le Coarer, S. Blaize, P. Benech, I. Stefanon, A. Morand, G. Léronnel, G. Leblond, “Wavelength-scale stationary-wave integrated Fourier-transform spectrometry,” *Nature Phot. (London)* **1**, 473–478 (2007).

11. F. Malbet, P. Kern, I. Schanen-Duport, J.-P. Berger, K. Rousselet-Perraut and P. Benech, "Integrated optics for astronomical interferometry – I. Concept and astronomical applications," *Astron. Astrophys. Suppl. Ser.* **138**, 135–145 (1999).
12. M. Ollivier and J.-M. Mariotti, "Improvement in the rejection rate of a nulling interferometer by spatial filtering," *Appl. Opt.* **36**, 5340–5346 (1997).
13. B. Mennesson, M. Ollivier and C. Ruilier, "Use of single-mode waveguides to correct the optical defects of a nulling interferometer," *J. Opt. Soc. Am. A* **19**, 596–602 (2002).
14. P. Klocek, *Handbook of infrared optical materials* (Marcel Dekker inc., 1991).
15. J.-P. Berger, P. Benech, I. Schanen-Duport, G. Maury, F. Malbet and F. Reynaud, "Combining up to eight telescope beams in a single chip," *Proc. SPIE* **4006**, 986 – 995 (2000).
16. A. W. Snyder and J. D. Love, *Optical waveguide theory* (Chapman and Hall, 1983).
17. D. L. Lee, *Electromagnetic Principles of Integrated Optics* (John Wiley and Sons Ltd., 1986).
18. L. Labadie, C. Vigreux-Bercovici, A. Pradel, P. Kern, B. Arezki, and J.-E. Broquin, "M-lines characterization of selenide and telluride waveguides for mid-infrared interferometry," *Opt. Express* **14**, 8459–8469 (2006).
19. M. Benisty, J.-P. Berger, L. Jocu, F. Malbet, K. Perraut, P. Labeye, and P. Kern, "The VSI/VITRUV combiner: a phase-shifted four-beam integrated optics combiner," *Proc. SPIE* **6268**, 62682D (2006).
20. E. Garmire, T. McMahon and M. Bass, "Propagation of infrared light in flexible hollow waveguides," *Appl. Opt.* **15**, 145–150 (1976).
21. E. Garmire, E., T. McMahon and M. Bass, "Flexible infrared waveguides for high-power transmission," *J. Quantum Electron.* **QE-16**, 23–32 (1980).
22. F. E. Vermeulen, C. R. James and A. M. Robinson, "Hollow microstructural waveguides for propagation of infrared radiation," *J. Lightwave Technol.* **9**, 1053–1060 (1991).
23. R. Bernini, S. Campopiano and L. Zeni, "Silicon micromachined hollow optical waveguides for sensing applications," *IEEE J. Sel. Top. Quantum Electron.* **8**, 106–110 (2002).
24. A. Bjarklev and J. Broeng, *Photonic crystal fibres* (Kluwer Academic Publishers, 2004).
25. T. A. Birks, J. C. Knight and P. St. J. Russell, "Endlessly single-mode photonic crystal fiber," *Opt. Lett.* **22**, 961–963 (1997).
26. S. E. Barkou, J. Broeng and A. Bjarklev, "Silica-air photonic crystal fiber design that permits waveguiding by a true photonic bandgap effect," *Opt. Lett.* **24**, 46–48 (1999).
27. S. Vergnole, L. Delage, F. Reynaud, L. Labonté, P. Roy, G. Mélin, and L. Gasca, "Test of photonic crystal fiber in broadband interferometry," *Appl. Opt.* **44**, 2496–2500 (2005).
28. S. Vergnole, L. Delage, and F. Reynaud, "Three-beam photonic crystal fiber imaging interferometer," *Appl. Opt.* **45**, 6712–6717 (2006).
29. J. S. Sanghera and I. D. Aggarwal, *Infrared fiber optics* (CRC Press, 1999).
30. P. Borde, G. Perrin, T. Nguyen, A. Amy-Klein, C. Daussy, P.-I. Raynal, A. Leger and G. Maze, "10- $\mu\text{m}$  wavefront spatial filtering: first results with chalcogenide fibers," *Proc. SPIE* **4838**, 273–279 (2003).
31. L. K. Cheng, A.-J. Faber, W. Gielesen, C. Boussard-Pledel, P. Houizot, J. Lucas, and J. Pereira Do Carmo, "Test results of the infrared single-mode fiber for the DARWIN mission," *Proc. SPIE* **5905**, 59051F-1–59051F-8 (2005).
32. A. Ksendzov, O. Lay, S. Martin, J. S. Sanghera, L. E. Busse, W. H. Kim, P. C. Pureza, W. V. Q. Nguyen, and I. D. Aggarwal, "Characterization of mid-infrared single-mode fibers as modal filters," *Appl. Opt.* **46**, 7957–7962 (2007).
33. V. Artiouchenko, ART Photonics, *Optical fibre and fabrication technique for an optical fibre*, European Patent EP/01.09.00/EP 00250290 (2000).
34. R. Flatscher, O. Wallner, V. Artjuschenko, and J. Pereira do Carmo, "Manufacturing of chalcogenide and silver-halide single-mode fibres for modal wavefront filtering for Darwin," *Proc. 6th Internat. Conf. on Space Optics* (2006).
35. S. Shalem, A. Tsun, E. Rave, A. Millo, L. Nagli, and A. Katzir, "Silver halide single-mode fibers for the middle infrared," *Appl. Phys. Lett.* **87**, 091103-1–091103-3 (2005).
36. T. Luo, S. Jiang, G. Nunzi Conti, S. Honkanen, S. B. Mendes, and N. Peyghambarian, "Ag<sup>+</sup>/Na<sup>+</sup> exchanged channel waveguides in germanate glass," *Electron. Lett.* **34**, 2239–2240 (1998).
37. J. Grelin, A. Bouchard, E. Ghibaud, and J. E. Broquin, "Study of Ag<sup>+</sup>/Na<sup>+</sup> ion-exchange diffusion on germanate glasses: Realization of single-mode waveguides at the wavelength of 1.55 $\mu\text{m}$ ," *Mater. Sci. Eng. B* **149**, 190–194 (2008).
38. Y. Ruan, W. Li, R. Jarvis, N. Madsen, A. Rode, and B. Luther-Davies, "Fabrication and characterization of low loss rib chalcogenide waveguides made by dry etching," *Opt. Express* **12**, 5140–5145 (2004).
39. S. J. Madden, D.-Y. Choi, D. A. Bulla, A. V. Rode, B. Luther-Davies, V. G. Taeed, M. D. Pelusi, and B. J. Eggleton, "Long, low loss etched As<sub>2</sub>S<sub>3</sub> chalcogenide waveguides for all-optical signal regeneration," *Opt. Express* **22**, 14414–14421 (2007).
40. C. Vigreux-Bercovici, E. Bonhomme, A. Pradel, J.-E. Broquin, L. Labadie, and P. Kern, "Transmission measurement at 10.6  $\mu\text{m}$  of Te<sub>2</sub>As<sub>3</sub>Se<sub>5</sub> rib waveguides on As<sub>2</sub>S<sub>3</sub> substrate," *Appl. Phys. Lett.* **90**, 011110–011112 (2007).

41. L. Labadie, *Nulling interferometry, integrated optics, infrared instrumentation, extrasolar planets; PhD dissertation* (Université Joseph Fourier, 2005).
42. N. Hô, M. C. Phillips, H. Qiao, P. J. Allen, K. Krishnaswami, B. J. Riley, T. L. Myers, and N. C. Anheier, "Single-mode low-loss chalcogenide glass waveguides for the mid-infrared," *Opt. Lett.* **31**, 1860–1862 (2006).
43. O. Eyal, S. Shalem and A. Katzir, "Silver halide midinfrared optical fiber Y coupler," *Opt. Lett.* **19**, 1843–1845 (1994).
44. U. J. Wehmeier, M. R. Swain, C. Y. Drouet D'Aubigny, D. R. Golish, and C. K. Walker, "The potential of conductive waveguides for nulling interferometry," *Proc. SPIE* **5491**, 1435–1445 (2004).
45. L. Labadie, P. Labeye, P. Kern, I. Schanen, B. Arezki, and J.-E. Broquin, "Modal filtering for nulling interferometry. First single-mode conductive waveguides in the mid-infrared," *Astron. Astrophys.* **450**, 1265–1275 (2006).
46. R. Flatscher, O. Wallner, and V. Artiouchenko, *Single-mode fibres for DARWIN*, Summary Report, ESA/ESTEC Contract No. AO/1-4023/01/NL/CK (2007).
47. E. Rave, K. Roodenko, and A. Katzir, "Infrared photonic crystal fiber," *Appl. Phys. Lett.* **83**, 1912–1914 (2003).
48. L. N. Butvina, O. V. Sereda, E. M. Dianov, N. V. Lichkova, and V. N. Zagorodnev, "Single-mode microstructured optical fiber for the middle infrared," *Opt. Lett.* **32**, 334–336 (2007).
49. L. Abel-Tiberini, L. Labadie, B. Arezki, P. Kern, R. Grille, P. Labeye, and J.-E. Broquin, "Transmission behaviors of single-mode hollow metallic waveguides dedicated to mid-infrared nulling interferometry," *Opt. Express* **15**, 18005–18013 (2007).
50. A. J. Faber, L. K. Cheng, W. L. M. Gielesen, C. Boussard-Pledel, S. Mauriceon, B. Bureau, X. H. Zhang, J. Lucas, and J. Pereira Do Carmo, "Optical characterization of infrared telluride glass fibers for space use," *Proc. Internat. Conf. on Space Optics* (2008).
51. G.L. Clark and C. Roychoudhuri, "Interferometry through single-mode optical fibers", *Proc. SPIE* **192**, 196–203 (1979).
52. D. Marcuse, *Principles of optical fiber measurements* (Academic Press, Inc. 1981).
53. O. Wallner, V. Artjuschenko and R. Flatscher, "Development of silver-halide single-mode fibers for modal filtering in the mid-infrared," *Proc. SPIE* **5491**, 636–646 (2004).
54. L. Labadie, E. Le Coarer, R. Maurand, P. Labeye, P. Kern, B. Arezki, and J.-E. Broquin, "Mid-infrared laser light nulling experiment using single-mode conductive waveguides," **471**, 355–360 (2007).
55. E. Laurent, K. Rousselet-Perraut, P. Benech, J.-P. Berger, S. Gluck, P. Haguenuer, P. Kern, F. Malbet, and I. Schanen-Duport, "Integrated optics for astronomical interferometry. V. Extension to the K band," *Astron. Astrophys.* **390**, 1171–1176 (2002).
56. P. Haguenuer and E. Serabyn, "Deep nulling of laser light with a single-mode-fiber beam combiner," *Appl. Opt.* **45**, 2749–2754 (2006).
57. C. Buisset, X. Rejeaunier, Y. Rabbia, and M. Barillot, "Stable deep nulling in polychromatic unpolarized light with multiaxial beam combination," *Appl. Opt.* **46**, 7817–7822 (2007).
58. F. Brachet, *Study and development of an achromatic phase shifter for nulling interferometry; PhD dissertation* (Université Paris XI, 2005).
59. V. Weber, M. Barillot, P. Haguenuer, P. Kern, I. Schanen-Duport, P. Labeye, L. Pujol, and Z. Sodnik, "Nulling interferometer based on an integrated optics combiner," *Proc. SPIE* **5491**, 842–849 (2004).
60. R. Flatscher, Z. Sodnik, K. Ergenzinger, U. Johann, and R. Vink, "Darwin Nulling Interferometer Breadboard I: System Engineering And Measurements," in *Towards Other Earths - Darwin/TPF and the Search for Extrasolar Terrestrial Planets*, M. Fridlund, ed. (ESA-SP, 2003), pp. 283.

## 1. Introduction

### 1.1. Scientific drivers for mid-infrared astronomy

Any celestial object with a non-zero temperature emits infrared radiation (i.e. heat). Because the wavelength at which the object most intensively radiates depends on the temperature, observing in the spectral range that goes from  $1\ \mu\text{m}$  to  $1000\ \mu\text{m}$  gives access to objects at a wide range of temperatures from a few tens of degrees Kelvin to several thousands. Although spectral boundaries are not firmly set, the region from  $1\ \mu\text{m}$  to  $5\ \mu\text{m}$  is defined as the near-infrared, from  $5\ \mu\text{m}$  to  $\sim 30\ \mu\text{m}$  we refer to the mid-infrared domain (or *thermal* infrared), while the far-infrared extends up to  $1000\ \mu\text{m}$ . The mid-infrared becomes a highly interesting observing regime, where warm objects with temperatures of  $\sim 100\text{--}600\ \text{K}$  can be probed. This corresponds to a temperature range where physical conditions for liquid water are encountered. It is also the range of peak emission of telluric planets around solar-type stars and therefore an appropriate domain for detecting the self-emission of nearby exoplanets. Furthermore, bio-markers such as water,  $\text{CO}_2$  or  $\text{O}_3$  (ozone) can be revealed through low-resolution spectroscopic observations. Mid-

infrared sources have become unquestionably a powerful source of information for relatively new fields like astrobiology and astrochemistry.

### 1.2. *Photonics, a recent technology for astronomy*

New technologies have constantly played a key role in improving the performance of astronomical instruments. With technology advancing at a rapid rate, future projects like the *E-ELT* (European Extremely Large Telescope), multi-aperture imaging or space-based infrared interferometry require us to fully reconsider the approach adopted so far for classical instruments. This can be justified by the high level of complexity of the classical solutions, the requirement of unprecedented performance or the need for reducing physically the size of future instruments. In this context, photonics can undoubtedly help to face some of this challenge. In the last decade, there has been an increasing and innovative use of photonic devices in astronomy. Optical fibers, the simplest photonics elements, are now commonly used for fiber-fed spectrographs in the visible. In the specific area of stellar interferometry, single-mode optical fibers are valuable for their spatial filtering capabilities, which help improving the accuracy on the interferometric visibilities [1]. Fibers are currently used on various interferometers like CHARA [2] or AMBER/VLTI [3] and will be implemented in future instruments to interconnect telescopes separated by a few hundred meters distance [4]. Beside optical fibers, Integrated optics (IO) is very promising for next generation multi-aperture interferometers since it offers the possibility of combining several beams in a single chip, leading to obvious advantages in terms of space and stability. This concept was implemented in the past on the IOTA interferometer [5, 6], and is foreseen to be part of the VLTI second generation instrumentation [7, 8]. This is the prelude to a valuable miniaturization of the interferometric instrumentation, possibly extending it in the future to other instrument concepts like integrated spectrograph [9, 10]. Photonic devices could also be helpful in the context of space-based experiments, where simple designs, and reliable and stable components are absolutely necessary. This points are important in particular for future interferometric missions like *Darwin/TPF*, *Pegase* or *SIM*.

Photonics has several strong advantages from the instrumental point-of-view, which justifies the extension of the concept towards new wavelengths. Some of these aspects which have been described in detail in [11] deserve our interest. The compactness offered by photonics-based components is a major advantage in the context of large telescope instrumentation and multi-aperture interferometry: *integrated* features allows us to save space and weight, and at the same time reduces the overall instrumental complexity. Photonics components can be placed in direct contact with a cryostat window or a detector [10]; They allow flux transportation in a much easier way than long optical trains; They permit faster and simpler instrument upgrade when dealing with optical chips; *single-mode* fibers and integrated optics allow very accurate beam cleaning, thanks to spatial and modal filtering, which is an essential aspect of aperture synthesis and nulling interferometers [12, 13]; When the waveguide is placed in a chilled enclosure, its limited numerical aperture acts as a field stop, avoiding straylight entering the system from outside the acceptance cone. This is an advantage when operating in the infrared, where thermal background from nearby warm optics is very high.

From these different points, photonics appears very attractive in the context of instrument miniaturization. However, the strong telecom background of photonics has concentrated the technological effort in few narrow bands of the near-infrared spectrum, where fully mature technology is available. When considering longer wavelengths of the *astronomical* mid-infrared spectrum, photonics suffers from a significant technological gap, which results from a weak mastering of the materials production and manufacturing processes at these wavelengths. Promising efforts, mainly driven by the potential applications of photonics in fields like astronomy, chemistry and biophysics, are being made to reduce the gap. The increasing use of

photonic devices for astronomical instrumentation has led to the neologism *astrophotonics*.

## 2. Materials and concepts for mid-infrared photonics

### 2.1. Accessing the 10- $\mu\text{m}$ spectral range: materials selection

The selection criteria for materials are based on the transparency window and on the corresponding intrinsic and extrinsic losses within this window. The window borders are determined by absorption, both on the visible and mid-infrared part of the spectrum. The intrinsic losses depend only on the material structure and properties and represent the minimum expected losses. However, the presence of impurities and defects further degrades the transmission and these losses are generally more important. We then talk about extrinsic losses. In the particular case of silica in the telecommunications industry, the refinement of the manufacturing technology over several years has led to high level of purity and quality, which makes the material losses close to the intrinsic levels. The physical explanation for intrinsic losses are found in material electronic transitions, phonon interactions and free-carrier effects. The interested reader can refer to well-established reference books on optical and infrared materials [14]. The infrared materials that have been tested so far in the context of dielectric photonics devices are chalcogenide glasses, silver-halide glasses and zinc selenide components. Most of these are also transparent in the visible. This has to be considered in case the resulting components have to operate in an environment non-shielded from optical radiation. On the other hand, this offers an advantage for alignment. All these materials are transparent at least up to 11-12  $\mu\text{m}$ . Depending on the chemical composition and the stoichiometry, the transmission range can be extended up to 18–20  $\mu\text{m}$  for the chalcogenide and zinc selenide glasses, or even beyond for silver halide glasses. In addition to their intrinsic properties, other factors may influence the optical behavior of these materials. These are:

- mechanical stress: most infrared materials show a certain fragility and high sensitivity to shocks, which may complicate the manufacturing and polishing processes.
- chemical stability: some materials can absorb water vapor, which further affects their transparency. In some cases, vacuum operation is required.
- thermal stress: while fibers are sensitive to temperature, integrated optics are generally more stable with regard to thermal constraints [15].
- spatial homogeneity: when a large surface is required to manufacture complex devices, it is important to ensure a good degree of homogeneity of the optical properties over the whole sample. Underestimating this aspect might bring in differential effects (dispersion etc...) that must then be carefully controlled.

Infrared glasses are typically classified in amorphous and crystalline forms, depending on the regular (crystalline) or irregular (amorphous) arrangement of the atomic structure.

Amorphous materials include oxide glasses (e.g.  $\text{SiO}_2$ ) which present strong absorption in the mid-infrared due to OH vibration modes. Other members of this group are chalcogenide glasses (based on S, Se and Te). The transmission of these materials can be extended beyond 12  $\mu\text{m}$  by the addition of heavy compounds (Ag, Te).

Crystalline materials show a regular pattern in their structure (e.g. Quartz, the crystalline form of  $\text{SiO}_2$ ). Silver halides – bromide or chloride – are also crystalline materials well known in mid-infrared applications. Semiconductors, also classified in this category, are attractive materials due to their extended transmission range in the infrared.

So far, chalcogenide and silver halide glasses are the two main materials that have been investigated to cover the mid-infrared range. Typical chalcogenide glasses are  $\text{As}_2\text{Se}_3$  and  $\text{As}_2\text{S}_3$ , which present good transparency up to  $\sim 12\text{--}16 \mu\text{m}$ . Compositions including Germanium (Ge)



or Tellurium (Te) can extend the transmission range up to  $20\ \mu\text{m}$ . Silver halide glasses have excellent transparency up to and beyond  $20\ \mu\text{m}$ . In terms of materials properties, silver halide glasses may encounter corrosive risks if in contact with metals. Furthermore, they present photosensitive properties, which require particular care if this effect is undesirable. On the other hand, the material photosensitivity can also be exploited for controlled laser writing of waveguides (see Sect. 3.1.2).

## 2.2. Waveguide concepts

### 2.2.1. Optical fibers and integrated optics

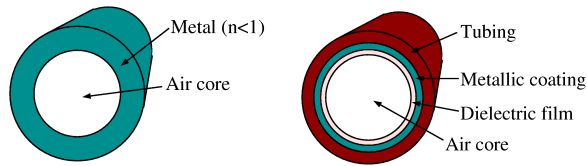
These types of dielectric waveguide represent a natural choice for developing guided optics for the mid-infrared, since they represent a spectral evolution of near-infrared concepts. We raise here only those issues which are important for the rest of the paper. For a detailed study of optical fibers and integrated optics principles, the reader can refer to classical references [16, 17]. Several refractive index profile can be considered when designing optical fibers: single-step index profile, double-step index profile, and smooth profile. The opto-geometrical parameters of the fiber (core and cladding size, refractive index difference  $\Delta n$ ) have a strong influence on the transmission range, the field confinement (strong or weak) or the numerical aperture. Most relevant for some astronomical applications are single-mode fibers. An important parameter to measure modal behavior is the normalized frequency of the fiber  $V = 2\pi\rho/\lambda(n_{co}^2 - n_{cl}^2)^{1/2}$  with core radius  $\rho$  and wavelength  $\lambda$  to be compared to the first order cut-off frequency  $V_c = 2.405$ . Depending on the index profile of the fiber, the single-mode bandwidth can be theoretically infinite (single-step index and smooth profiles) or finite (double-step index fibers under certain conditions on the cladding index).

As for classical fibers, *planar* dielectric integrated optics confines the light by total internal reflection. The main difference with fibers is on the waveguide geometry and on a stiff and fixed arrangement of the waveguides on the substrate surface. The basic brick is the slab waveguide, whose modal properties are governed by the dispersion equation of the slab waveguide [18]. An integrated optics chip can gather within a small glass surface a high number of optical functions. It becomes a very powerful solution for interconnecting interferometrically several telescopes and obtaining accurate phase-shifted outputs for measuring visibilities [19]. Non-linear crystals such as Lithium Niobate ( $\text{LiNbO}_3$ ) are used to build active components, such as electro-optic modulators with high accuracy phase control. The combination of integrated optics beam combiners and dispersing elements (e.g. AWG or Arrayed Waveguide Gratings) could lead to promising end-to-end integrated instruments with unprecedented mechanical stability. In practice, as for many photonic device, integrated optics chips present a certain number of limitations on their wide spread use in astronomy. The effective bandwidth of operation is generally narrow and the optical functions are highly wavelength dependent. Cross-talk effects between different channels can degrade the useful signal, although this can be reduced by a careful design of the chip.

### 2.2.2. Hollow waveguides and photonic-crystal fibers

Hollow waveguides were initially proposed as an alternative to dielectric fibers because of the lack of core infrared materials with suitable structural properties. In hollow waveguides, infrared radiation propagates in ideal low-loss media like air or vacuum thanks to specular reflections on the metal-coated walls of the structure. Following the first experimental demonstration of this concept [20, 21], a large variety of hollow waveguides has been developed based on the air-core multi-layer structure. Two main class of hollow waveguides can be distinguished (see Fig. 1): hollow metallic waveguides (HMW) are made of metallic tubes or metallic layers deposited inside a micromachined structure. Because of the specular nature of the electromagnetic

### Hollow waveguides



### Photonic crystal fibers

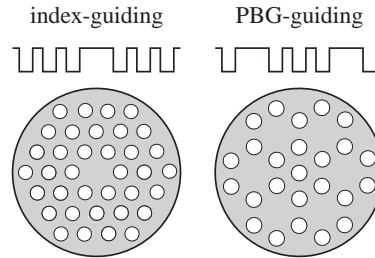


Fig. 1. Left: principles of hollow metallic waveguides and hollow glass waveguides. In the HGW design, the tubing can be glass or a plastic polymer. Right: refractive index profiles of index-guiding and photonic bandgap (PBG) guiding PCF.

wave reflection, there is no limiting entrance angle as in dielectric fibres. Imperfect reflectivity and roughness of the coating are responsible for propagation losses. A second class is hollow glass waveguides (HGW) or hollow plastic waveguides (HPW) for which glass – or plastic – tubing is used with an internal multi-layer dielectric-metallic coating. In this case, leaky modes are confined by the underlying metallic coating. HGW present lower losses over a broader spectral range compared to HMW, due to a smoother inner wall. Circular waveguides with core diameter from  $200\ \mu\text{m}$  to  $1000\ \mu\text{m}$  are commonly found, but they are highly multimode and not compliant with the single-mode property required in some astronomical applications. Because of the importance of single-mode behavior for several applications, some authors have theoretically investigated the modal behavior in hollow waveguides with various geometries and emphasized the conditions for single-mode behavior [22, 23]. This led to the identification of quasi single-mode circular waveguides and strictly single-mode rectangular waveguides. Such single-mode waveguides are quite lossy with attenuation around  $\sim 30\ \text{dB/m}$ , which limits their use to short propagation lengths. The typical cross-section dimensions of *single-mode* waveguides is of the order of one to two wavelengths, i.e.  $10$  to  $20\ \mu\text{m}$  in the mid-infrared range. It is only recently that micro-machining capabilities permitted the production of hollow waveguides at this scale, allowing fruitful synergies between microwave engineering and infrared photonics. Photonic crystal fibers (PCF) are made of dielectric structures with periodically varying refractive index at the wavelength scale [24]. These structures exhibit photonic bandgaps, which are frequency intervals within which light propagation is forbidden in certain directions. PCF are formed from a dielectric rod containing tubes of a material of lower refractive index or air, arranged in a special pattern and running along the fiber axis. Two types of photonic crystal fibers may be distinguished: those with an index-guiding structure and those with a photonic bandgap-guiding structure (see Fig. 1). The pattern of air or low refractive index tubes determines the waveguiding properties. Single-mode operation is possible for both types of PCFs, although with different single-mode bandwidth and different propagation properties: – Index-guiding PCFs are formed by a not necessarily periodic structure of air or low refractive index tubes at wavelength scale, embedded in some dielectric material. A defect which confines the light and therefore acts as the core is introduced by omitting one tube. Waveguidance can be explained by considering that the cladding region provides (due to the tubes) an effective index which is smaller than the core index. Depending on the wavelength, the effective index approaches the material index of the core, if the field is mainly guided within the material, or the index of the tubes, if the field penetrates the cladding. With the effective cladding index approach, the index-guiding PCF can be modeled as a single-step index fiber with an effec-

tive normalized frequency of  $V_{eff} = \pi\Lambda/\lambda(n_m^2 - n_{eff}^2)^{1/2}$ , where the core diameter is given by the center-to-center spacing  $\Lambda$  between two adjacent tubes. In contrast to conventional single-step index fibers,  $V_{eff}$  approaches a constant value for large  $\Lambda/\lambda$ . This means that by proper choice of the hole diameter to hole spacing ratio  $d/\Lambda$ , such a fiber can be single-mode for any wavelength [25].

– Photonic-bandgap (PBG) guiding PCFs are obtained by locally breaking the periodicity of a photonic crystal by introducing a well-defined defect, e.g. in the form of an extra tube. The light then is confined and thus guided, provided that the surrounding photonic crystal cladding exhibits a photonic bandgap at the operation wavelength [26]. A remarkable difference between PBG-guiding PCFs and conventional fibers or index-guiding PCFs is that they allow waveguidance with propagation constants (i.e. photonic bandgaps) below the effective cladding index. The photonic bandgap regions, i.e. the transmission windows, are determined by the cladding structure only. They are usually very narrow. The behavior of the guided modes within the photonic bandgaps is solely determined by the characteristic of the defect. By varying the size and shape of the defect, the frequency of the guided mode can be positioned precisely within a photonic bandgap. At near-infrared wavelengths, substantial work has led to the implementation of PCF in astronomical applications [27, 28].

### 3. Overview of development activities

#### 3.1. Manufacturing techniques

##### 3.1.1. Optical fibers

**Chalcogenide glass fibers:** The manufacturing techniques for optical fibers are determined by the the different physical properties of fiber materials. In the mid-infrared we distinguish between glassy fibers and crystalline fibers. For both types, a preform is created by mechanical combination of the core and cladding material. Glassy fibers are drawn from the preform, whereas crystalline fibers are extruded from the preform.

Chalcogenide glass was the first material used to produce mid-infrared fibers. A two or more-component glass is formed by combining one or more chalcogene elements such as sulphur, selenium or tellurium with one or more elements such as arsenic, germanium, phosphorus, antimony, gallium, aluminum or silicon. The properties of the glass change drastically with composition. In general, chalcogenide glasses are very stable, durable, and insensitive to moisture. A distinctive difference between these and other mid-infrared fiber glasses is that they do not transmit well in the whole visible region and that their refractive indices are quite high. Arsenic-Trisulfide ( $As_2S_3$ ) fibers have a transmission range from 0.7 to about 12  $\mu m$ . Longer wavelengths can be transmitted by adding heavier elements like Tellurium, Germanium or Selenium. Chalcogenide glass formation can be achieved when the chalcogenide elements are melted and quenched in an evacuated silica glass ampoule with one or more elements as mentioned above. After heating in a rocking furnace for longer than 10 hours at a temperature between 700 and 900°C, the ampoule is quenched in air and annealed to room temperature. The preform is fabricated by using rod-in-tube (core rod is placed within the cladding tube) or casting methods (melted core material is cast into the cladding rod). The two methods in use for fiber drawing are preform drawing and crucible drawing. In the case of fibers with no glass cladding or only a polymer cladding, e.g. teflon, the conventional preform drawing method with a tube furnace and a narrow heat zone within an inert gas atmosphere is used. Fibers with chalcogenide cladding are drawn in a similar apparatus. The core rod and cladding tubes are placed into a silicon muffle furnace, zonally heated, and drawn into a fiber. Core-cladding fibers can also be produced by a double-crucible technique or by modified crucible drawing, a technique offering the advantages of both crucible drawing and preform drawing



[29]. Single-mode fibers made of chalcogenide glass have been and are currently developed for ESA and NASA in the framework of the planned missions DARWIN and TPF-I. The fibers are intended as spatial wavefront filters for the wavelength range from about 4 to 12  $\mu\text{m}$ . **Several** independent research activities demonstrated the feasibility of single-mode fibers: – A team at LESIA (Observatoire de Paris, France) and Le Verre Fluoré (France) developed a single-mode fiber of chalcogenide glass for spatial wavefront filtering [30]. The fiber had a core/cladding composition of  $\text{As}_2\text{Se}_3/\text{Ge}_2\text{SeTe}_{1.4}$  with a numerical aperture of 0.15 and core and cladding diameters of 40  $\mu\text{m}$  and 210  $\mu\text{m}$ , respectively. – A team at TNO (The Netherlands) and the University of Rennes (France) developed for ESA several samples of chalcogenide fibers by different preform manufacturing methods, including internal rotational casting, fiber or rod in tube vacuum. Single-mode operation has been demonstrated for a fiber composed of Te-As-Se glass with a core diameter of 22  $\mu\text{m}$ , a cladding diameter of 500  $\mu\text{m}$ , core and cladding refractive indices of 2.927 and 2.924, and a nominal single-mode cutoff wavelength of 3.7  $\mu\text{m}$  [31]. In a second activity the team is analyzing tellurium-based chalcogenide fibers for the use in the wavelength range from about 10 to 20  $\mu\text{m}$ . Mono-index fiber samples with compositions of Te-Ge-Ga-I, Te-Ge-I and Te-Ge-Se have been produced with diameters in the range of 400 to 550  $\mu\text{m}$ . Because the properties of Tellurium-based glass depend on temperature, the fiber samples show improved transmission at cryogenic temperatures. – The Naval Research Laboratory (United States) developed for NASA chalcogenide glass single-mode fibers for use at wavelengths up to about 11  $\mu\text{m}$ . The fibers had a core diameter of 23  $\mu\text{m}$ , a cladding diameter of 127  $\mu\text{m}$ , and core and cladding refractive indices of 2.725 and 2.714 [32].

**Silver-Halide Fibers** Crystalline materials have the advantage of a better long wavelength transmission compared to mid-infrared glasses, but suffer from a difficult fabrication process. The first crystalline fibers were made of hot extruded KRS-5 (Tellurium-Bromide-Iodide). Today, poly-crystalline silver-halide (Silver-Chloride-Bromide) is most widely used. Silver-halide fibers show good transmission up to almost 20  $\mu\text{m}$ . Poly-crystalline fibers are made of crystal-like solid solutions of Thallium halides, e.g. KRS-5, or silver halides, e.g. AgClBr. These materials offer such properties as ductility, low melting point, and isotropy. Crystalline fibers can be fabricated via plastic deformation by extrusion from a preform. The rod-in-tube preform is realized by a rod of AgClBr as core and a Cl-rich AgClBr crystal as cladding. The preform can also be made by the casting method or by preform growth methods [33]. The preform is placed in a heated chamber and the fiber is extruded to its final form through a polished die. Typical extrusion temperatures are in the range of 50% to 80% of the melting temperature, which is 457°C for AgCl, for example. The pressure within the container ranges from a few to some ten tons per square centimeter. Similar to the chalcogenide glass fibers, poly-crystalline silver-halide fibers have been and are currently being developed for ESA and NASA. Two independent research activities demonstrated the feasibility of single-mode fibers: – A team at Astrium GmbH (Germany) and ART Photonics (Germany) developed for ESA several samples of silver-halide fibers with different core/cladding geometries and different material compositions [34]. To achieve optimum results, extremely homogeneous crystals have been used and different preform manufacturing techniques have been applied, including mechanical combination, preform growth, capillary drop and capillary suction. Single-mode operation has been successfully demonstrated at a wavelength of 10.6  $\mu\text{m}$  for a fiber with a core/clad composition of  $\text{AgCl}_{75}\text{Br}_{25}/\text{AgCl}_{60}\text{Br}_{40}$ , a core diameter of 20  $\mu\text{m}$ , a cladding diameter of 500  $\mu\text{m}$ , and a single-mode cutoff wavelength of 5.8  $\mu\text{m}$ . In a second activity, the team is currently developing single-mode fibers by an improved and reproducible manufacturing process to obtain fibers with improved performance. The test setup is extended and allows interferometric measurements at wavelengths of 5.3  $\mu\text{m}$ , 10.6  $\mu\text{m}$  and 16.5  $\mu\text{m}$  to verify the performance over almost

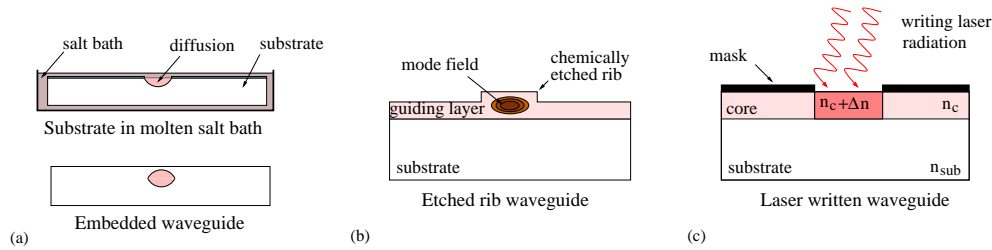


Fig. 2. Schematic view of the three main technologies for manufacturing integrated optics

the entire wavelength range. – A team at Tel Aviv University (Israel) developed for NASA silver-halide fibers for TPF-I. An improved crystal growth technique allowed inhomogeneities of less than 2% for preforms of any composition. An improved fiber has been developed with a double-step index profile. The core composition was  $\text{AgCl}_{30}\text{Br}_{70}$ , the composition of the first cladding  $\text{AgCl}_{32}\text{Br}_{68}$  and that of the second cladding  $\text{AgCl}_5\text{Br}_{95}$ . The core diameter was  $50\ \mu\text{m}$ , the diameter of the first cladding  $250\ \mu\text{m}$  and that of the second cladding  $900\ \mu\text{m}$  (see Fig. 3 and [35]). The outer cladding was blackened by exposure to UV radiation.

### 3.1.2. Integrated Optics

While Integrated Optics is a well mastered technology below  $2\ \mu\text{m}$ , the situation is noticeably different at longer wavelengths. The manufacturing techniques need to be adapted to infrared materials with different structural, mechanical and thermal properties, like high fragility. Possible technologies for manufacturing integrated optics are based on ion-exchange, waveguide chemical etching and photo-darkening.

**Ion-exchange diffusion** In the ion-exchange technique, a glass substrate is first layered with a few hundred nanometers of polysilicon coating with diffusion apertures obtained by ion etching (see Fig 2(a)). The structure is then placed in a molten salt bath with precisely determined ion concentrations and treatment duration. The difference in concentration results in local ion exchange from the bath to the substrate, producing the high index core embedded in the substrate. In the mid-infrared range, this technique has been successfully implemented on Germanate glasses for the  $3\text{--}4\ \mu\text{m}$  spectral range, although the experimental characterization has so far been limited to a wavelength of  $1.55\ \mu\text{m}$  [36, 37].

**Chemical etching under controlled atmosphere** The chemical etching technique is among the most promising solutions to work with amorphous glasses like chalcogenide (see Fig 2(b)). Dry etching has already produced rib waveguides based  $\text{As}_2\text{S}_3$ ,  $\text{As}_2\text{Se}_3$  and Germanium components which were characterized at  $1.5\ \mu\text{m}$  [38, 39]. Later, analog rib waveguides were obtained using Tellurium compounds and characterized at  $10.6\ \mu\text{m}$  (see Fig. 4 and [40]). The first step in the manufacturing process is the deposition of a guiding layer by means of thermal evaporation or sputtering, followed by optical characterization [18]. These two processes influence the film parameters such as density, refractive index and surface roughness. A mask with the waveguide pattern is realized before undergoing chemical etching in Argon or  $\text{CF}_4/\text{O}_2$  atmosphere. The process produces sharp, well defined waveguide contours, with step resolution better than  $0.1\ \mu\text{m}$ . Some authors have demonstrated the feasibility of bent waveguides, which is an important prerequisite for more complex integrated optics functions [39]. Chemical etching has been also attempted on crystalline glass compounds for slab waveguides made of a Zinc Selenide ( $\text{ZnSe}$ ) film deposited on a Zinc Sulfide ( $\text{ZnS}$ ) substrate [41]. However, the chemical

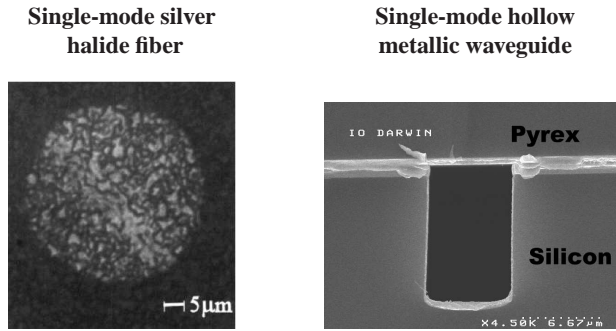


Fig. 3. Left: cross section of a single-mode silver halide fiber characterized by output profile imaging [35]. Right: photograph of a conductive waveguide cross-section with dimensions  $10 \times 5 \mu\text{m}$ . This structure maintains a single polarization direction perpendicular to the longer side [45].

and mechanical stability of the structure could not be preserved during the etching phase, and the layer was irretrievably damaged.

**Photo-darkening effect and laser writing** A third way of producing mid-infrared integrated optics is to use the photo-darkening effect for amorphous glasses (see Fig 2(c)). Photo-darkening results from exposure of the substrate to high-power external radiation, in order to modify locally the refractive index of the glass. Although the correlation between photo-darkening effect and structural changes in the substrate is not well understood, it has been observed that photo-darkening occurs only in disordered amorphous materials, and not in crystalline materials. The process of waveguide manufacturing using the photo-darkening effect is named *laser writing*. This consists in focusing a visible source such as He-Ne laser in a particular location of the substrate surface leading to a change in the refractive index, which amplitude is a function of the exposure time to the radiation. This technique has been successfully applied to the As-S-Se family of chalcogenide glasses. Based on this technique, some authors could obtain a square cross-section single-mode waveguide with  $5.4 \mu\text{m}$  width and  $\Delta n \sim 0.04$  using laser writing at 632 nm [42]. This work has been done in the continuation of Efimov et al. (2001) effort to obtain analog results with 850 nm laser writing. We wish also to underline that, depending on the exposition conditions, the photo-darkening effect can be reversible or permanent.

**Impact factors towards single-mode behavior** Beyond the manufacturing aspects of channel waveguides, the possibility to achieve single-mode behavior depends on the capabilities of manufacturing small cores (i.e.  $< 10 \mu\text{m}$ ). This implies a higher refinement and mastering of the various technological parameters. Alternatives to planar dielectric integrated optics exist to produce functions: a possibility is to emulate the near-infrared fiber couplers as this was done by Eyal et al. (1994) who mechanically joined uncladded  $900\text{-}\mu\text{m}$  core silver-halide fibers to produce a Y-coupler for the mid-infrared [43]. Another option is to downgrade microwave E-plane and H-plane coupler to the  $10\text{-}\mu\text{m}$  range as suggested by Wehmeier et al. (2004) [44]. However, obtaining a single-mode Y-coupler would require the handling of much smaller cores, while the solution of conductive waveguides needs additional developments to reduce the linear losses. Furthermore, the level of integration appears in both cases lower compared to planar integrated optics.

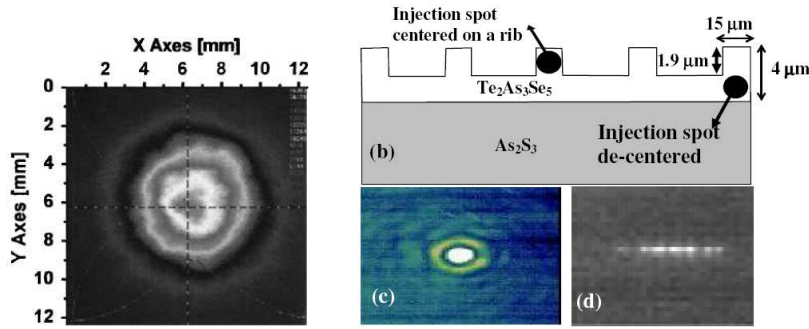


Fig. 4. Left: output profile of a 2.2-m long single-mode silver halide fiber obtained at  $10.6\ \mu\text{m}$  [35]. Right: sketch of a chalcogenide rib waveguide showing the position of the injection spot, together with output images at  $10.6\ \mu\text{m}$  when the spot is centered and de-centered from the rib [40].

### 3.1.3. Hollow waveguides

While a certain amount of theoretical work has been produced to investigate the properties of *single-mode* hollow waveguides for the mid-infrared range, little has been done from the experimental approach. Single-mode hollow waveguides have been limited by the actual micrometer capabilities of micro-machining techniques. Recently, different groups have addressed this manufacturability aspect. The group at Steward Observatory (Arizona) involved in radio and sub-mm instrumentation has tested the manufacturing of conductive waveguides by laser micromachining. This consists in etching a silicon wafer with high power (30 W) Argon laser in order to obtain a preform. These wafers are then gold coated, bonded and cut to obtain the waveguides. The accuracy and quality of the laser etching process is of crucial importance to realize the samples and minimize their losses. At the time of their published work [44], the group could not achieve better than a  $6\ \mu\text{m}$  resolution, which is compatible with operation in the 2-THz ( $150\ \mu\text{m}$ ) regime. A second group based in Grenoble (France) has investigated a similar idea, but based on well mastered chemical etching process of the silicon wafer. The advantage is to obtain smaller structures with sizes down to  $4\ \mu\text{m}$  and 50–100 nm resolution, together with smoother waveguide walls. The deposited gold layer shows then a more uniform surface, which reduces scattering. The studied waveguide concept was inspired from well-known microwave rectangular waveguides, but scaled down to typical sizes of  $\sim 10\ \mu\text{m}$ . Hollow metallic waveguides with rectangular geometry and with cross-section dimensions of  $10 \times 5\ \mu\text{m}$  were produced with this technique and characterized at  $10.6\ \mu\text{m}$  (see Fig. 3 and [45]). Later, Y-junctions based on hollow metallic waveguides were also manufactured, but with no sufficient transmission in the mid-infrared spectral range.

### 3.1.4. Photonic crystal fibers

The manufacturing techniques for photonic crystal fibers are similar to that for optical fibers and therefore are determined by the fiber materials. PCFs made of glassy material are drawn from the preform, PCFs made of crystalline material are extruded from the preform. The major difference with optical fibers is given by the preform fabrication technique. It shall be noted that PCFs for the mid-infrared are at a very experimental stage today. For glassy PCFs the preform is usually obtained by drilling holes in the fiber material. For crystalline PCFs the preform cannot be obtained by drilling holes in the preform as these would be destroyed during the extrusion process. A reduced effective cladding index is obtained by adding a material of

lower index to the cladding region [46]. A one-dimensional photonic crystal is achieved by alternately coiling thin layers of silver-chloride and silver-bromide on a central silver-bromide rod. Two dimensional photonic crystals are achieved by filling the holes in a silver-bromide rod with small rods of silver-chloride, or by stacking silver-chloride and silver-bromide core-only fibers around a central rod of silver-bromide.

Experimental PCFs made of silver-halide have been manufactured by several groups. The first index-guiding PCF was drawn from a preform realized by stacking core/clad fibers around an uncladded AgBr fiber [47]. The fiber showed an effective core diameter of  $200\ \mu\text{m}$ . Other fibers have been realized from a silver-halide preform made of  $\text{AgCl}_{20}\text{Br}_{80}$  with holes drilled in a hexagonal pattern [48]. The holes are filled with rods made of  $\text{AgCl}_{50}\text{Br}_{50}$ . The extruded fiber showed a hole to distance spacing of  $d/\Lambda = 0.74$ , an effective core diameter of  $79\ \mu\text{m}$  and a numerical aperture of 0.16.

### 3.1.5. Considerations on design and technology

In the context of astronomy, photonics devices face a certain number of requirements linked to the original design of astronomical instruments, both from the design and technology point-of-view. For instance, classical optics (lens, mirrors...) used to feed an instrument are slow optics, with high numerical aperture that does not match one of fibers or integrated optics. This requires to use tapers, which in return can introduce additional losses if they are not adiabatic. Another point concern the importance of facet cleaning and anti-reflection coatings to limit Fresnel losses at the waveguide input. This is a technological aspect which is not yet very well accounted for, especially for mid-infrared waveguides. A trade-off between these different considerations is essential in the astronomical context, where transmission losses have to be kept as low as possible.

## 3.2. *Testing techniques and characterization results*

### 3.2.1. Transmission range and excess losses

Transmission range and losses are the two fundamental parameters that define and fix the operability of the waveguides in the range of interest. The combined effect of transmission range and losses is very strongly dependent on the material, the applied technological process and the waveguides geometry. This measurement is the first step of any characterization phase. – In the case of dielectric waveguides, the transmission range simply refers to the spectral domain where photons are not absorbed by the material. Obviously, this definition is linked to the transparency window of the bulk material. The effective transmission range is provided through spectroscopy measurements in the region of interest. For dielectric bulks, the transparency window is obtained by FTIR spectroscopy, which is a standard technique and will not be further developed here. – Excess losses regroup propagation losses, coupling losses and Fresnel losses. Excess losses are specific to each waveguide and directly depending on its opto-geometrical parameters (length, numerical aperture, index difference at air-waveguide interface). The different contributions to excess losses are difficult to disentangle for a single waveguide. Overall excess losses can be measured in dedicated Fourier Transform spectroscopy experiments in which light is launched into the waveguide placed in the optical path. In some cases, it is possible to extract separately coupling and propagation losses by differential measurements on similar waveguides with different lengths and numerical aperture. This method is also named “cut-back method”. This method gives good results, but requires then a dedicated set of waveguides planned in the manufacturing phase [49]. Measurement campaigns on the different type of waveguides presented in Sect. 3.1 have shown a relatively large span in the measured losses. Chalcogenide and silver-halides fibers show the best transmission, even in single-mode regime, with losses at  $10\ \mu\text{m}$  of 8 dB/m [32], 10 to 18 dB/m [31], 20 dB/m [30], 23.2 dB/m [34], 25 dB/m [35]. Ex-



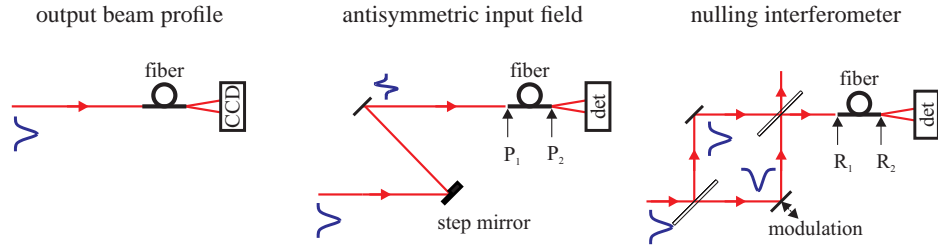


Fig. 5. Measurement procedures to verify single-mode behavior and spatial filtering of optical fibers. See text for details.

perimental measurements at longer wavelengths for chalcogenide fibers have led to increased values up to 40 dB/m between 12 and 13  $\mu\text{m}$ , and 150 to 300 dB/m between 16 to 20  $\mu\text{m}$  [50]. Dielectric integrated optics have presented so far higher losses in the range of 1 to 10 dB/cm [40, 42]. However, integrated optics is designed to operate over much shorter propagation distances than fibers. At this stage of the development of mid-IR waveguides, the reason of the high dispersion in the propagation losses is mainly found in the non-optimized manufacturing processes (impurities, defects etc...). More exotic waveguides like PCFs and hollow waveguide show a quite different behavior. In two cases, mid-infrared photonic-crystal fibers have shown very different losses of  $\sim 2$  dB/m [48] and 60 dB/m [47], but the single-mode behavior is not assessed. For hollow waveguides as well, we found a strong dispersion in the performance. For most multimode mid-infrared hollow waveguides, straight losses can be as low as few dB/m, which is attractive for power transportation. However, single-mode hollow waveguides are less advanced technologically, and the first prototypes have shown high losses of several dB/mm [45]. Understanding such a discrepancy requires further advances from the technological side.

### 3.2.2. Single-mode regime and spatial filtering

Supporting only a single spatial mode is a key feature of optical fibers for astronomical applications, and especially for mid-infrared interferometry [51]. For mid-infrared fibers, one may think on different procedures which rely either on measuring the fibers' far field intensity distribution or on measuring the fibers waveguiding properties (see Fig. 5). The procedures differ clearly in complexity and accuracy:

- The straightforward method is to measure the fiber output beam profile at discrete wavelengths. If it corresponds to the field distribution as expected from theory and if it does not change in shape when changing the input beam launch conditions or when bending the fiber, the fiber can be assumed to be single-mode. The output beam profile can either be measured with an infrared camera or by scanning with a single-pixel detector. From the fiber divergence angle, the normalized frequency  $V$  can be directly deduced [52]. Due to the limited accuracy, measuring the fiber output beam profile provides only a qualitative assessment.
- Because the fundamental mode of a single-mode fibers is symmetric with respect to the fiber axis, the single-mode behavior and the spatial filtering capabilities can be investigated by launching an antisymmetric beam into the fiber [32]. If the fiber is purely single-mode, no signal can theoretically be measured at the fiber output. Any leakage signal at the fiber output is due to higher-order modes, back-reflection of cladding modes, or to a not perfectly antisymmetric input field. The ratio of leakage power  $P_2$  to the incident power  $P_1$  may serve as a qualitative metric. A simple way for realizing an antisymmetric field is a step-like mirror. The required antisymmetry of the input field is the limiting factor for this method.
- Spatial wavefront filtering with single-mode fibers is of particular importance in nulling interferometry for equalizing the transverse field

distributions in order to achieve high rejection ratios. Such interferometric test setup can therefore be used to verify the single-mode behavior and the spatial filtering capability [53, 54]. For instance, the rejection ratio (constructive to destructive interference power) of a Mach-Zehnder interferometer is supposed to be much higher when employing a single-mode fiber at its output ( $R_2$ ) compared to the rejection ratio achievable without the fiber ( $R_1$ ). The ratio  $R_2/R_1$ , also called filter action, serves as a quality metric for the improvement in the rejection ratio. All measurements suffer from residual light guided in the cladding. This is significant for mid-infrared fibers, which have usually short length due to the high attenuation. Absorbing coatings are therefore mandatory for those astronomical applications that rely on the mode purity. Furthermore, aperture masks may be applied at the fiber entrance or exit. However, their achromaticity has to be taken into account for broadband applications. As an alternative to monochromatic characterization methods, it is also possible to detect modal cut-off wavelengths in the waveguide spectrum as less power is transported with increasing wavelength. It is then possible to identify in this way single-mode, bimode, trimode regions etc... This method, commonly applied in the near-infrared [55], is more delicate to implement in the mid-infrared because of the lack of bright blackbody sources. However, coupling the detection chain with a high-sensitivity MCT single-pixel detector and a lock-in detection provides a sufficient signal-to-noise gain to measure mid-infrared calibrated spectra through the waveguide [41]. Low-loss waveguides obviously help in increasing the experimental SNR. Eventually, evidence of single-polarization in the case of hollow rectangular waveguides can be exploited to demonstrate at a given wavelength the single-mode nature of the waveguides. This method has been successfully applied to assess the modal behavior at  $10.6\ \mu\text{m}$  of the rectangular samples shown in Fig. 3. Among the mid-infrared waveguide prototypes presented in Sect. 3.1, chalcogenide and silver-halide fibers had single-mode behavior tested through output field imaging and consequent qualitative fitting to the Gaussian profile of the fiber fundamental mode (see Fig. 4 and [30, 31, 35]). In the other cases, nulling interferometry techniques were used to measure a high order modes rejection ratio of about  $1000\pm 300$  [32] and a filter action  $R_2/R_1=400$ . The modal behavior of integrated optics waveguides has been up to now assessed by output field imaging. In the last ten years, there has been a strong improvement in the measurement of the absolute rejection ratio obtained thanks to modal filtering through several experiments in the visible, near and mid-infrared. Several teams in Europe and in the U.S. have been working on nulling interferometry based on single-mode waveguides improving rejection ratios up to  $10^4$  to  $10^6$ , depending on the wavelength range and bandwidth [56, 54, 57, 58, 59, 60], and getting very close to the requirement of  $10^5$  broadband rejection ratio in the mid-infrared. Note that other nulling experiments based on bulk optics setup provided very deep null, but they are not presented here since they do not have photonic devices implemented.

#### 4. Conclusions and perspectives

We presented in this paper an overview of the research activities in the field of mid-infrared astrophotonics. The effort from different groups has concentrated mainly on the development of single-mode waveguides like fibers and integrated optics. Many dielectric-based solutions explored for the mid-infrared are inspired from near-infrared concepts, like step-index and graded-index fibers. Other concepts like hollow waveguides, which are specifically designed to operate beyond  $2\text{--}3\ \mu\text{m}$  and that do not have strong applications in the telecom bands, have been investigated with some success. Integrated optics at mid-infrared wavelengths is also emerging with the development of single-mode channel waveguides manufactured on planar waveguides. Photonics crystal fibers are part of a new generation of promising waveguides, but it should be acknowledged that PCFs for the mid-infrared are still at an experimental level. Single-mode behavior has been successfully demonstrated experimentally for different technologies, ultimately

through nulling interferometry experiments where the measured quantity is the extinction ratio of the source light. Two hard points appear to be limiting factors for mid-infrared photonics: the first one concerns the high losses measured for these structures. However, this is mainly resulting from the non-optimized manufacturing techniques, which increasing maturity in the next years will help to improve the performance. The second point concerns the relative narrow bandwidth of the developed waveguides when compared to the astronomical needs. The experimental characterization has been often limited to a narrow wavelength range around  $8.4\ \mu\text{m}$  or  $10.6\ \mu\text{m}$ . Broadband characterization will help in the future to better answer to astronomical requirements. Although mid-infrared photonics has not reached yet the level of maturity obtained in near-infrared, the results of the last five to ten years are promising and open the way to new perspectives.

Some concern the short-term improvement of the existing technologies. In particular, the demonstration of planar integrated channel waveguides is a key step towards first optical functions like beam combination. Furthermore, single-mode mid-infrared fibers have shown very good filtering properties in the context of nulling interferometry, which will be probably further improved in the coming years. In the long-term, while fibers appear as a rapidly maturing technology for mid-infrared stellar interferometry, integrated optics could be the ideal technology for instrumentation that requires to combine several optical functions. In particular, considering the future ELTs – *Extremely Large Telescopes* – integrated optics could have spectroscopic capabilities included within the same optical chip [10], which is certainly of a major interest for facilities growing in size and cost. Eventually, beyond the frame of astrophotonics, mid-infrared photonics presents applications in the field of chemical and biological sensors, which makes them even more attractive for the next decades.

### **Acknowledgments**

The authors thank the anonymous referee for his useful comments to improve the scientific quality of the paper. The authors also thank Dr. T. M. Herbst for the constructive discussions and the accurate reading of the paper. LL gratefully acknowledges the funding support from the Max-Planck-Gesellschaft (MPG).